X-ray magnetic-circular-dichroism probe of a noncollinear magnetic arrangement below the spin reorientation transition in $Nd_2Fe_{14}B$

Jesús Chaboy, Luis M. García, and Fernando Bartolomé*
Instituto de Ciencia de Materiales de Aragón and Departamento de Física de la Materia Condensada, CSIC-Universidad de Zaragoza, 50009 Zaragoza, Spain

Augusto Marcelli and Giannantonio Cibin
I. N. F. N., Laboratori Nazionali di Frascati - C. P. 13, 00044 Frascati, Italy

Hiroshi Maruyama
Department of Physics, Faculty of Science, Okayama University, Japan

Stefania Pizzini
Laboratoire L. Neel, CNRS, Boîte Postale 166X, 38042 Grenoble Cedex, France

Andrei Rogalev, Jeroen B. Goedkoop, and José Goulon
ESRF, Boîte Postale 220, 38042 Grenoble Cedex, France
(Received 21 July 1997)

The experimental detection of a spin reorientation phase transition by means of Fe K-edge x-ray magnetic circular dichroism (XMCD) is reported for $Nd_2Fe_{14}B$. The temperature dependence of the XMCD signals at both Fe (K edge) and Nd ($L_{2,3}$ edges) is compared to that of the mutual orientation of the Fe and Nd magnetic moments derived from macroscopic magnetic measurements. The present study results in the experimental probe of the existence of a noncollinear arrangement of both Fe and Nd magnetic moments, throughout the spin reorientation transition. [S0163-1829(98)06213-4]

I. INTRODUCTION

After many years of a great activity in the 1960s and the 1970s, a new start in the permanent magnet research field came from the discovery of the $R_2Fe_{14}B$ intermetallic compounds.[1,2] Due to its large economical consequences in the huge market of permanent magnets, a great deal of basic research was focused on $Nd_2Fe_{14}B$, which exhibits superior high-performance permanent-magnet properties over the earlier Sm-Co materials. This compound has a tetragonal crystal structure belonging to the space group $P4_2/mnm$. While at room temperature the magnetic anisotropy is clearly uniaxial, favoring the [001] direction as the easy magnetization direction, single-crystal studies of its magnetic properties revealed that $Nd_2Fe_{14}B$ exhibits a spin reorientation transition (SRT) at $T_s \sim 135$ K. As this SRT transition sets in, the magnetization begins to deviate from the **c** axis when decreasing the temperature below T_s.[3,4] The occurrence of such a transition destroys the uniaxial anisotropy and worsens its performance for technological applications. When this spin reorientation was first observed, one of the questions which arose was whether or not there was a canting of the rare-earth and iron spins relative to one another in the low-temperature phase or whether they remained basically collinear as in the high-temperature phase.[5] Initially, it was derived from magnetization measurements of $Nd_2Fe_{14}B$ single crystals that the magnetization tilts from the **c** axis at temperatures above T_s towards the [110] axis at lower temperatures, and that the tilt angle of the total magnetization reaches 30.6° at 4.2 K.[6] However, ^{57}Fe Mössbauer studies show that the iron hyperfine field tilts at 4.2 K by only 27°.[7] These results indicate that below T_s the Nd sublattice magnetization is not oriented parallel to the iron sublattice magnetization. Despite the large body of research aimed at determining the mutual orientation of the Nd and Fe moments throughout the spin reorientation transition, no general consensus has been reached so far. Indeed, theoretical calculations based on magnetization analyses predict that the average Nd moment is within 2–3° collinear with the Fe sublattice magnetization.[8] On the contrary, combined magnetization and ^{57}Fe Mössbauer,[7] polarized neutron,[9] ^{145}Nd Mössbauer spectroscopy,[10] and x-ray resonant magnetic scattering[11] studies conclude that the arrangement between the Nd and Fe magnetic moments can be considerably noncollinear in the low-temperature phase.

The complicated interplay of exchange and crystal-field interactions in the $R_2Fe_{14}B$ series has triggered numerous studies. Even nowadays, there is a continuing effort to determine the magnetic structure of $Nd_2Fe_{14}B$ as a fundamental step to understand the role of the different interactions into determining the intrinsic magnetic properties of the $R_2Fe_{14}B$ compounds.[12] We have designed a x-ray magnetic circular dichroism (XMCD) experiment trying to solve the puzzle concerning the magnetic arrangement of $Nd_2Fe_{14}B$ in the low-temperature phase. The XMCD spectroscopy allows direct measurement of the spin-dependent absorption cross section on a given atomic species in a material with net magnetization.[13] XMCD probes the spin polarization of the empty states of a given symmetry near the Fermi level by selecting the initial state. In this way, by recording the Fe

K-edge XMCD it is possible to probe the spin polarization of the Fe $4p$ states and the conduction band, through the strong Fe($4p$,$3d$)-R($5d$) hybridization, whereas the L_2 absorption probes the spin-polarized $5d$ empty density of states at the rare-earth sites. Therefore, the characteristic element and shell selectivities of XMCD offers a unique opportunity to monitor the temperature dependence of the angular arrangement of both, Fe and Nd magnetic moments in $Nd_2Fe_{14}B$.

In a previous investigation we reported the experimental observation of a SRT by using x-ray magnetic circular dichroism at the Nd L_2 edge in a $Nd_2Fe_{14}B$ polycrystalline sample.[14] However, notwithstanding that the capability of XMCD to study SRT processes was well established, the constraint of using powdered samples prevented us going further on the analysis, that was limited to the Nd L_2 edge. Here, we present an extended experiment improved by the use of single-crystal specimens and by optimization of the experimental setup. Then, XMCD at the Fe K edge and at the Nd $L_{2,3}$ edges has been applied to study the spin reorientation transition in a $Nd_2Fe_{14}B$ single crystal. Our aim here is (i) to demonstrate on one hand, the feasibility of XMCD in the hard x-ray range to study magnetic order-order phase transitions, even at the Fe K edge whose relative magnetic contribution is in the order of only 10^{-3} compared to the amplitude of the spin-averaged absorption, (ii) to obtain a deeper insight into the magnetic changes occurred at a microscopic scale, triggering the SRT. Furthermore, the combined analysis of the XMCD at both Nd and Fe sites will provide a better understanding of the relationship between the integrated XMCD signals involving delocalized final states and the local magnetic moments in intermetallics systems.

II. EXPERIMENTAL

A $Nd_2Fe_{14}B$ single-crystal grown by Sagawa was used for the XMCD experiments.[15] The [110] direction of the single crystal is perpendicular to a polished face of 6×4 mm. Magnetization measurements were carried out to verify both the spin reorientation transition temperature (at about 135 K), and the coercive field of the specimen (less than 0.4 T).

The XMCD experiments at the Fe K edge and at the Nd $L_{2,3}$ edges were carried out at the ESRF beamline ID12A which is dedicated to polarization-dependent x-ray-absorption studies.[16] The source is the helical undulator HELIOS II which emits x-ray radiation with a high polarization rate of above 90% and flexible polarization (circular left–circular right). The second harmonic of the undulator spectrum was selected to cover the range from 6 to 9 keV. The fixed-exit double-crystal monochromator was equipped with a pair of Si(111) crystals cooled down to $-140°$ C. The circular polarization rate of the undulator radiation was estimated to be about 90%.[16]

XMCD signals were obtained through the difference of x-ray-absorption near-edge structure (XANES) spectra recorded consecutively either by reversing the helicity of the incident beam or by flipping the magnetic field ($\sim$ of about 1 T) generated by a superconducting electromagnet and applied along the beam direction. The XANES spectra were recorded at different fixed temperatures in the fluorescent

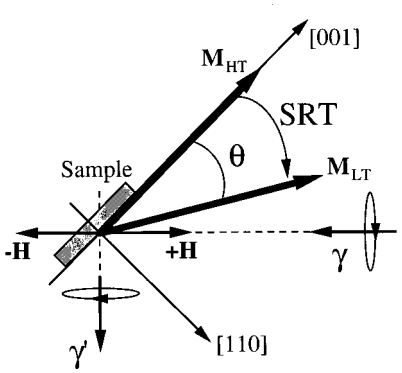

FIG. 1. Schematic view of the (horizontal) scattering plane. The sample is mounted in such a way that [001] and [110] directions form a 45° angle with the incident beam (γ) direction, in which the alternating magnetic field ($\pm$H) is applied. The spin reorientation transition tilts the easy axis of the macroscopic magnetization from its high-temperature direction given by M_{HT} to M_{LT}, forming a continuously increasing theta angle with the c axis towards the [110] direction as the SRT sets in. The XANES spectra are measured field by recording the fluorescence (γ') at a 90° scattering angle.

detection mode using a Si photodiode associated with a digital lock in exploiting the modulation of the x-ray beam.[17] The sample was mounted with the incident plane tilted 45° away from the beam direction, so that both the [001] and [110] directions form a 45° angle, within the orbit plane, with the incident beam. A detailed scheme of the experimental setup is shown in Fig. 1.

The spin-dependent absorption coefficient was obtained as the difference of the absorption coefficient $\mu_c=(\mu^- - \mu^+)$ for antiparallel, μ^-, and parallel, μ^+, orientation of the photon helicity and the magnetic field applied to the sample. The spectra were normalized to the averaged absorption coefficient at high energy, μ_0, in order to eliminate the dependence of the absorption on the sample thickness, so that $\mu_c(E)/\mu_0=[\mu^-(E)-\mu^+(E)]/\mu_0$ corresponds to the dimensionless spin-dependent absorption coefficient. It is important to note that no correction for self-absorption has been performed during the analysis. The comparison between the current XMCD spectra and those recorded in the transmission mode assures that no modification of the shape is induced on the spectra by self-absorption.[14,18] Moreover, to avoid any amplitude reduction that can be attributed to self-absorption effects, we have limited ourselves to a temperature dependence XMCD analysis relative to the high-temperature XMCD spectra.

III. RESULTS AND DISCUSSION

The XMCD spectra were recorded at different (13) temperatures, ranging between $T=20$ K and room temperature, at both the Fe K edge and the Nd $L_{2,3}$ edges in $Nd_2Fe_{14}B$ single crystal. The working temperatures were selected in order to closely follow the evolution of XMCD through the spin reorientation transition. We show in Fig. 2 some representative spectra recorded at different temperatures at both Fe and Nd absorption edges. The shapes of the XMCD spectra are similar to those previously reported for $Nd_2Fe_{14}B$. However, the amplitudes of the dichroic signals are consid-

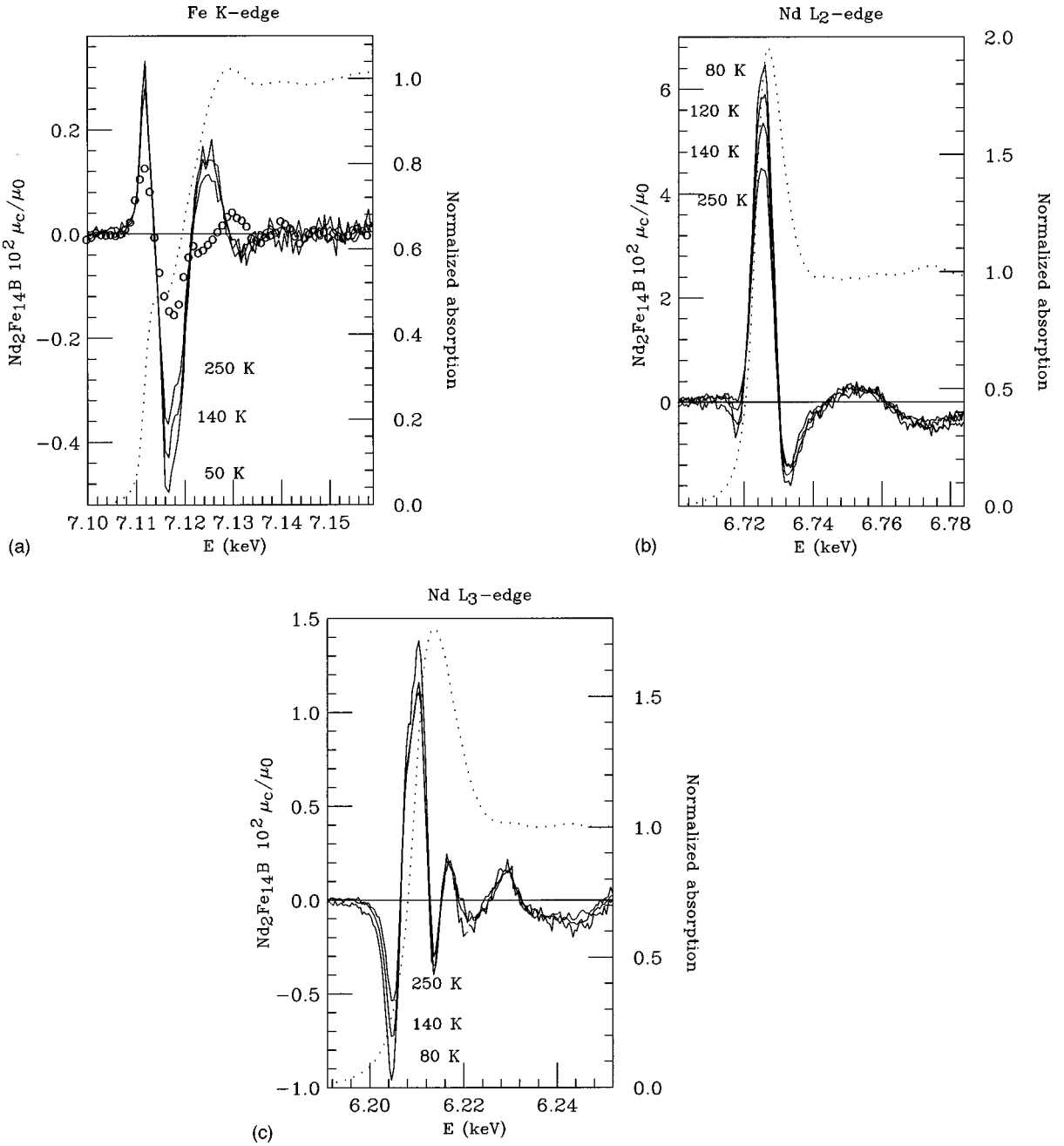

FIG. 2. Normalized XMCD spectra ($\times 10^2$) recorded at different temperatures at the different absorption edges in the $Nd_2Fe_{14}B$ single crystal: (a) Fe *K* edge, (b) Nd L_2 edge, and (c) Nd L_3 edge. In all the cases, the spin-averaged absorption recorded at 250 K is also shown (dots). In panel (a) the Fe *K*-edge XMCD of elemental iron is reported for sake of comparison (○).

erably higher than those obtained under the same conditions on polycrystalline samples. Indeed, it has been reported that the amplitude of the XMCD is ~0.15% and ~2% at the Fe *K* edge and at the Nd L_2 edge, respectively.[16] These results were obtained at room temperature by measuring a Nd-Fe-B block at the same beamline and under the same experimental conditions as the measurements that we present here. However, we have carried out the experiments on a single-crystal specimen and we find that the amplitude of the XMCD signal is ~0.45% for Fe *K* edge and ~2.8% for Nd L_2 edge. It should be also noted that the single-crystal Fe *K* edge XMCD signal at room temperature in $Nd_2Fe_{14}B$ is about twice as large as that of elemental iron. The huge increase of the XMCD amplitude is undoubtedly linked to the use of a single-crystal sample, that guarantees single magnetic domain conditions in our XMCD experiments. This result points out the need of using optimized samples to prevent the reduction of the XMCD due to the existence of different magnetic domains within the sample or the effect of misorientation of grains in polycrystalline materials, that prevents both the full saturation and full reversion of the magnetization under the action of the external magnetic field.

The shape and the sign of the XMCD signals at the different absorption edges, shown in Fig. 2, are consistent with those previously reported for *R*-Fe intermetallic compounds in which *R* is a light rare-earth and the iron sublattice determines the sign of the magnetization.[14,19,20]

The model commonly adopted to account for the mag-

netic coupling between Fe and R sublattices in such a class of intermetallic compounds is due to Campbell.[21] This model considers that the R-Fe interaction is determined by the $R(5d)$-Fe$(3d)$ hybridization that renders antiparallel the $3d$ and $5d$ spins. As the rare-earth intra-atomic $4f$-$5d$ exchange interaction renders parallel the $4f$ and $5d$ spins, both Fe$(3d)$ and $R(4f)$ spins are antiparallel. Then, as $\mathbf{J}=\mathbf{L}-\mathbf{S}$ ($\mathbf{J}=\mathbf{L}+\mathbf{S}$) for light (heavy) rare-earths, the R and Fe magnetic moments are ferromagnetically (antiferromagnetically) coupled for light (heavy) rare-earth compounds.

In the case of $Nd_2Fe_{14}B$, as the temperature is decreased through the spin reorientation transition, no modification of the XMCD shape or sign is detected, indicating that no change of the magnetic coupling takes place during the SRT. However, the change in intensity of the main positive peak in the dichroic signal is about 40, 50, and 30% for K, L_2, and L_3 edges, respectively.

These results show how XMCD is sensitive to the spin reorientation transition. Therefore, the next step in our study is to analyze the temperature dependence of the different signals in order to determine their relationship with both the magnitude and angular dependence (referred to the crystallographic **c** axis) of the local magnetic moments in the compound, μ_{Fe} and μ_{Nd}. To this end we have considered the integrated intensity of the XMCD as a function of temperature. In the case of both L_2 and L_3 Nd edges, the main positive peak of the XMCD signals has been integrated and the result, scaled by subtracting the 250 K value from all the others, is reported in Fig. 3. The integrals have been limited to these regions because according to a recent resonant inelastic x-ray-scattering investigation performed at the rare-earth L edges on the $R_2Fe_{14}B$ series, the main positive XMCD peak corresponds to a dipolar excitation, whereas for lower energies there is a quadrupolar channel which dominates the XMCD spectra.[22] In both Nd L_2 and L_3 edges, the amplitude of the integrated dichroic signal raises continuously as the temperature decreases, as shown in Fig. 3(a). Below 150 K there is a sharp increase of the signal down to 110 K. At this temperature the signal shows a rounded maximum and starts to decrease slowly as cooling down to the lowest measured temperature.

This behavior is consistent with the macroscopic second-order description of the spin reorientation transition, since around 135 K the magnetization tilts from the **c** axis towards [110] by an angle θ which increases continuously as the temperature decreases. Within this framework and according to our experimental setup (see Fig. 1), the projection of the magnetization on the x-ray beam direction starts to increase as the SRT sets on. Consequently, as the XMCD signal is directly related to this projection, the XMCD is expected to increase below the spin reorientation temperature. Moreover, it is important to note that the amplitude of both Nd L_2 and L_3 integrated XMCD signals scale through the whole temperature range. This result points to a single origin of the magnetic signal at the Nd $L_{2,3}$ edges, being due to the strong polarization of the Nd $5d$ states caused by the presence of a localized $4f$ magnetic moment at the Nd sites.

The analysis of the Fe K-edge signal has been made according to Ref. 18, in which a systematic study of the Fe K-edge XMCD through the $R_2Fe_{14}B$ series shows that the shape of the dichroic spectra is rare-earth dependent. Ac-

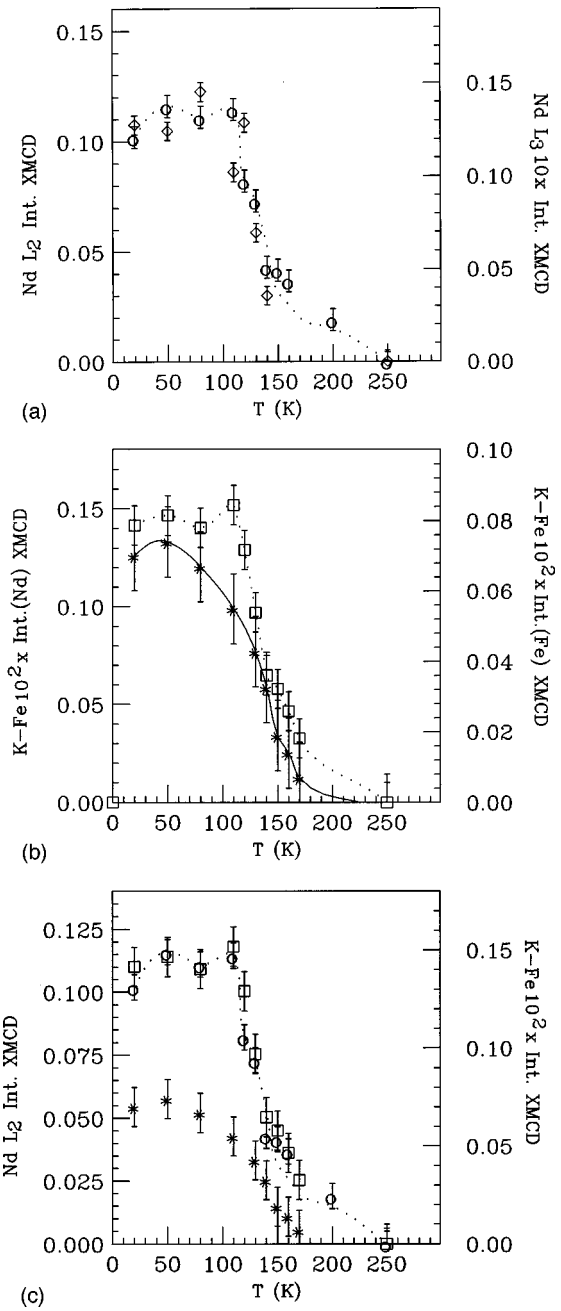

FIG. 3. (a) Comparison of the integrated XMCD signal at the Nd L_2 (○) and L_3 edges (◇) in $Nd_2Fe_{14}B$ as a function of temperature. The L_3-edge signal has been multiplied by a factor of 10. (b) Comparison of the temperature dependence of the integrated signals extracted from the Fe K-edge XMCD signal after the subtraction of the $Y_2Fe_{14}B$ XMCD signal: Nd-like (□), Fe-like (⋆) (see text for details). (c) Comparison between the temperature dependence of the integrated Nd L_2 XMCD signal (○) and those derived from the Fe K-edge XMCD after subtracting the $Y_2Fe_{14}B$ XMCD signal: Nd-like (□), Fe-like (⋆).

cording to this model, we have assumed that the total magnetization of the $R_2Fe_{14}B$ compounds is the addition of both iron and R sublattice magnetizations, and that the average magnetization of the Fe sublattice in the series is given by the magnetization of the $R=Y$ compound.[5,18] We have therefore considered that the Fe K-edge XMCD spectrum in Nd $_2Fe_{14}B$ corresponds to the addition of the magnetic contribu-

tion of both Fe and Nd sublattices, so that the remaining signal after the subtraction of the Fe K-edge XMCD signal of $Y_2Fe_{14}B$ would correspond to the Nd sublattice magnetic contribution. To analyze our data under this model, we have first subtracted the Fe K-edge XMCD signal of $Y_2Fe_{14}B$ from that of $Nd_2Fe_{14}B$, and then integrated the signal in two different energy ranges. The first one covers the region where the Fe K-edge signal exhibits, before subtraction, the characteristic sharp positive peak assigned exclusively to iron (referred to as Fe-like in the captions). The second range covers the remaining signal in the XMCD spectra, which is assumed to be due to the rare-earth sublattice magnetic contribution (referred to as a Nd-like in the captions).[18] The result of this procedure is shown in Fig. 3(b), where the integrated signals have been referred to the 250 K data by subtracting the 250 K value from all the others. From this figure it is clear how the two integrated signals reflect a different temperature dependence, as it can be expected as due to the Fe and Nd magnetic sublattices, respectively. Moreover, it has to be noted that the second signal extracted, whose origin is addressed to the rare-earth, can be exactly scaled to those obtained at the Nd $L_{2,3}$ edges, see Fig. 3(c), being in agreement with the hypothesis above, i.e., that the extracted contribution to the Fe K-edge XMCD signal reflects the magnetic state of the Nd atoms in this system through the Fe($4p$,$3d$)-R($5d$) hybridization.

The previous analysis advances the existing relationship between the XMCD signals at both Fe and Nd sites with the local magnetic moments μ_{Fe} and μ_{Nd}. Therefore, the study of their temperature dependence will lead to an atomic species-resolved determination of the angular dependence of the magnetic moments with respect to the **c** axis during the spin reorientation transition. Indeed, notwithstanding that the bulk magnetization behavior of $Nd_2Fe_{14}B$ has been well determined through macroscopic measurements, no general agreement on the evolution of the magnetic moments on the microscopic scale has been reached so far. As a result, different models involving collinear and noncollinear arrangements of the Fe and Nd moments in the low-temperature phase have been proposed.[7–11]

In order to obtain a deeper insight into this controversy, we have compared the temperature dependence of our XMCD spectra with the available data of $[\mu_{Nd}(T),\ \theta_{Nd}(T)]$, and $[\mu_{Fe}(T),\ \theta_{Fe}(T)]$, where θ is the canting angle with respect to the **c** axis, corresponding to the different proposed arrangements.[7–10] In Fig. 4(a) we show the comparison of the temperature dependence of the integrated Nd L_2-edge XMCD signal and the projection along the x-ray wave vector of the Nd magnetic moment obtained from Refs. 7 and 8, corresponding, respectively, to noncollinear and collinear arrangements of the Nd and Fe moments in the low-temperature phase. According to the noncollinear model derived by Onoedera *et al.*,[7] the values of θ_{Nd} and θ_{Fe} are found to be 58° and 27°, respectively, at 4.2 K. As clearly shown in Fig. 4, the best agreement is obtained when using the data of Ref. 7, i.e., by considering a noncollinear coupling of the Fe and Nd magnetic moments in the low-temperature phase, as well as a sudden increase of the Nd magnetic moment as the SRT sets on, this last being in agreement with ^{145}Nd Mössbauer spectroscopy results.[10] This analysis satisfactorily explains the measured XMCD

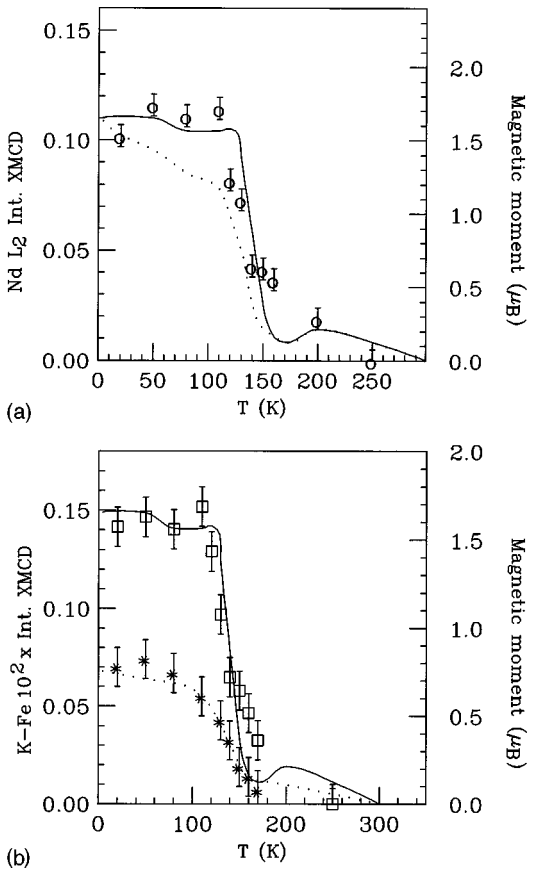

FIG. 4. (a) Comparison between the temperature dependence of the integrated Nd L_2-edge XMCD signal (○) and the projection along the x-ray wave vector of the Nd magnetic moment obtained from Ref. 7 (solid line) and Ref. 8 (dotted line) corresponding, respectively, to a noncollinear (collinear) arrangement of the Nd and Fe moments in the low-temperature phase. (b) Comparison between the temperature dependence of the integrated signals derived from the Fe K-edge XMCD after subtracting the $Y_2Fe_{14}B$ XMCD, [Nd-like (□), Fe-like (⋆)], and the projection along **k** of the μ_{Nd} (solid line) and μ_{Fe} (dotted line) magnetic moments taken from Ref. 7.

signals at the Nd $L_{2,3}$ edges. In the case of the Fe K-edge XMCD spectra this result is even more clear. In Fig. 4(b), the temperature dependence of the two integrated signals, (derived from the Fe K-edge XMCD after subtracting the $Y_2Fe_{14}B$ XMCD), corresponding to the magnetic contribution from the Fe and Nd sublattices, are compared, using the same scale, to $\mu_{Fe}(T)$ and $\mu_{Nd}(T)$ obtained from Ref. 7, i.e., by imposing an angular dependence involving a noncollinear arrangement between the two magnetic sublattices. As clearly shown in the figure, each integrated XMCD signal follows the temperature behavior of $\mu_{Fe}(T)$ and $\mu_{Nd}(T)$, thus supporting the existence of a noncollinear magnetic arrangement below the SRT in $Nd_2Fe_{14}B$, as well as the Fe K-edge signal being due to the addition of two components, associated to the magnetic contribution from the Fe and Nd sublattices, respectively.

IV. SUMMARY AND CONCLUSIONS

In this work, x-ray magnetic circular dichroism (XMCD) at the Fe K edge and at the Nd $L_{2,3}$ edges has been applied to

study the spin reorientation transition occurring in $Nd_2Fe_{14}B$ at temperatures below 135 K.

Our study demonstrates, on the one hand, the feasibility of XMCD to study magnetic order-order phase transitions even at the Fe *K* edge whose relative magnetic contribution is in the order of only 10^{-3} compared to the amplitude of the spin-averaged absorption. On the other hand, the analysis of the XMCD signals recorded at the different absorption edges has allowed us to determine the relative magnetic arrangement between the Fe and Nd sublattices in the low-temperature phase. Our data are consistent with the existence of a noncollinear arrangement of both Fe and Nd magnetic moments throughout the spin reorientation transition as proposed by Onoedera *et al.*,[7] i.e., the canting angles θ_{Nd} and θ_{Fe} reach 58° and 27°, respectively, at 4.2 K.

Finally, special attention has been devoted to the analysis of the Fe *K*-edge signals. Our study identifies, in agreement with our previously published results,[18] the influence of the Nd sublattice magnetization on the Fe *K*-edge XMCD spectrum. In the framework of a two-sublattice model, it is possible to extract the magnetic contribution of both Fe and Nd from the XMCD signal, each one showing a different temperature dependence that is in agreement with the noncollinear arrangement of both sublattices in the low-temperature phase.

ACKNOWLEDGMENTS

This work was partially supported by INFN-CICYT and LEA-MANES collaboration programs, and by Spanish DGICYT Grant No. MAT96-0448. The experimental work at the European Synchrotron Radiation Facility has been performed with the approval of the ESRF Program Advisory Committee (Proposal HC-543).

*Present address: Laboratoire de Cristallographie, CNRS, BP166 38042 Grenoble, France.

[1] M. Sagawa, S. Fujimura, N. Togawa, H. Yamamoto, and Y. Matsuura, J. Appl. Phys. **55**, 2083 (1984).

[2] J. J. Croat, J. F. Herbst, R. W. Lee, and F. E. Pinkerton, Appl. Phys. Lett. **44**, 148 (1984).

[3] D. Givord, H. S. Li, and R. Perrier de la Bathie, Solid State Commun. **51**, 857 (1984).

[4] M. Sagawa, S. Fujimura, H. Yamamoto, Y. Matsuura, and S. Hirosawa, J. Appl. Phys. **57**, 4094 (1985).

[5] For a review, see J. F. Herbst, Rev. Mod. Phys. **63**, 819 (1991), and references therein.

[6] K. Tokuhara, Y. Ohtsu, F. Ono, O. Yamada, M. Sagawa, and Y. Matsuura, Solid State Commun. **56**, 333 (1985).

[7] H. Onoedera, A. Fujita, H. Yamamoto, M. Sagawa, and S. Hirosawa, J. Magn. Magn. Mater. **68**, 6 (1987); **68**, 15 (1987).

[8] H. S. Li, Ph.D thesis, Grenoble, 1987; J. Cadogan, J. P. Gavigan, D. Givord, and H. S. Li, J. Phys. F **18**, 779 (1988).

[9] D. Givord, H. S. Li, and F. Tasset, J. Appl. Phys. **57**, 4100 (1985); quoted by D. Givord, H. S. Li, J. M. Moreau, and P. Tenaud, J. Magn. Magn. Mater. **54-57**, 445 (1986).

[10] I. Nowik, K. Muraleedharan, G. Wortmann, B. Perscheid, G. Kaindl, and N. C. Koon, Solid State Commun. **76**, 967 (1990).

[11] A. Koizumi, K. Namikawa, H. Maruyama, K. Mori, and H. Yamazaki, Jpn. J. Appl. Phys., Part 1 **32**, 332 (1993).

[12] Y. Yan, H. Jin, and T. Zhao, J. Magn. Magn. Mater. **164**, 201 (1996).

[13] G. Schütz, W. Wagner, W. Wilhelm, P. Kienle, R. Zeller, R. Frahm, and G. Materlik, Phys. Rev. Lett. **58**, 737 (1987).

[14] J. Chaboy, A. Marcelli, L. M. García, J. Bartolomé, M. D. Kuzmin, H. Maruyama, K. Kobayashi, H. Kawata, and T. Iwazumi, Europhys. Lett. **28**, 135 (1994).

[15] D. Givord, H. S. Li, J. M. Cadogan, J. M. D. Coey, J. P. Gavigan, O. Yamada, H. Maruyama, M. Sagawa, and S. Hirosawa, J. Appl. Phys. **63**, 3713 (1988).

[16] J. Goulon, N. B. Brookes, C. Gauthier, J. Goedkoop, C. Goulon-Ginet, M. Hagelstein, and A. Rogalev, Physica B **208&209**, 199 (1995).

[17] C. Gauthier, C. Goujoin, S. Feite, E. Moguiline, L. Braicovich, N. B. Brookes, and J. Goulon, Physica B **208&209**, 232 (1995).

[18] J. Chaboy, H. Maruyama, L. M. García, J. Bartolomé, K. Kobayashi, N. Kawamura, A. Marcelli, and L. Bozukov, Phys. Rev. B **54**, R15 637 (1996).

[19] J. Chaboy, L. M. García, F. Bartolomé, J. Bartolomé, H. Maruyama, K. Kobayashi, N. Kawamura, A. Marcelli, and L. Bozukov, J. Phys. IV **7**, C2-449 (1997).

[20] F. Baudelet, E. Dartyge, A. Fontaine, C. Brouder, G. Krill, J. P. Kappler, and M. Piecuch, Phys. Rev. B **43**, 5857 (1991).

[21] I. A. Campbell, J. Phys. F **2**, L47 (1972).

[22] F. Bartolomé, J. M. Tonnerre, L. Seve, D. Raoux, J. Chaboy, L. M. García, M. Krisch, and C. C. Kao, Phys. Rev. Lett. **79**, 3775 (1997).